Pressure effect on YBa2Cu3O7 thin film growth in offaxis radio frequency magnetron sputtering

S. C. Wu, W. C. Tsai, C. K. Huang, H. T. Hsu, C. J. Huang, and T. Y. Tseng

---

Articles you may be interested in

Atomic oxygen effect on the in situ growth of stoichiometric YBa2Cu3O7 epitaxial films by facing targets 90° off axis radiofrequency magnetron sputtering
J. Appl. Phys. **77**, 5809 (1995); 10.1063/1.359160

Formation of Curich particles on the surface of YBa2Cu3O7x thin film grown by in situ offaxis sputtering
J. Appl. Phys. **75**, 2020 (1994); 10.1063/1.356302

Relation between electrical properties and microstructure of YBa2Cu3O7x thin films deposited by singletarget off axis sputtering
J. Appl. Phys. **75**, 393 (1994); 10.1063/1.357012

Offaxis laser deposition of YBa2Cu3O7 thin films
Appl. Phys. Lett. **61**, 3178 (1992); 10.1063/1.107951

Offaxis sputter deposition of YBa2Cu3O7 thin films for microwave applications
Appl. Phys. Lett. **59**, 1629 (1991); 10.1063/1.106252

Pressure effect on YBa$_2$Cu$_3$O$_7$ thin film growth in off-axis radio frequency magnetron sputtering

S. C. Wu, W. C. Tsai, C. K. Huang, H. T. Hsu, C. J. Huang, and T. Y. Tseng
Department of Electronics Engineering and Institute of Electronics, National Chiao-Tung University, Hsinchu, Taiwan, Republic of China

YBa$_2$Cu$_3$O$_{7-x}$ (123) thin films were fabricated on (100) MgO substrates by off-axis single target radio frequency (rf) magnetron sputtering. Our study focused on the effect of chamber pressure on the composition, microstructure, and superconductive properties on transition behavior and T_c of the grown film studied. An empirical formula was derived to explain the dependence of the deposition rate of various components on the pressure. Next, we compared the transport mechanism of the sputtered particles between the off-axis rf and the on-axis direct current sputtering and determined the processing conditions that result in superconducting films of better quality. According to our findings, growth at higher pressures ($>$100 mTorr) produces more homogeneous and higher T_c superconducting films. © *1995 American Vacuum Society.*

I. INTRODUCTION

Applications of oxide superconductor devices require thin film growth techniques with higher reproducibility and reliability in order to obtain better surface morphology and higher quality superconducting films. Recently, various thin film growth techniques have been used for this purpose, including multiple-source electron beam evaporation,[1] ion beam sputtering,[2] molecular beam epitaxy,[3] pulsed laser ablation,[4] metalorganic deposition,[5] and direct current (dc)[6] or radio frequency (rf)[7–9] sputtering. Each of these techniques has its own unique features, such as large area growth, high growth rate, better surface morphology, or lower growth temperature. To meet the practical requirements of device fabrication simple growing equipment and simple processes are required. Hence, single target dc or rf sputtering methods are most attractive. However, using the sputtering technique to promote thin film growth of high T_c superconducting oxides results in energetic negative ion bombardment.[10–13] Bombardment caused by energetic particles may modify the film composition,[14] deteriorate the surface morphology,[15] induce some defects in the films,[16] and, in extreme cases, result in net etching rather than deposition.[14] Therefore, many methods have been developed to overcome the bombardment effect, including heavy compensation for the target composition for different sputtering yields at the substrate surface,[17] sputtering in high pressure[18] to slow down the energetic particles which increases the colliding probabilities and reduces the resputtering damage, and changing the configuration of the substrate to target in order to avoid direct substrate bombardment by energetic particles, i.e., an off-axis configuration system.[19]

In this article, we study the influence of growth chamber pressure on the metallic composition, the surface morphology, and the electrical properties of superconducting films grown by off-axis rf sputtering. We also derive an empirical formula that is based on the dependence of the relative atomic ratios of Ba to Y and Cu to Y on chamber pressure. After comparing these results with those obtained from dc on-axis sputtering and after investigating the transport mechanism of sputtered particles, we will provide a more complete discussion. The empirical formula may predict the relationship between metallic atom composition and pressure, and may be adopted to grow thin films with exact stoichiometry and better surface morphology.

II. EXPERIMENT

A rf off-axis sputtering system was used to grow the superconducting films. The substrates were polished (100) MgO single crystals vertically mounted onto the heater block with silver paste. The substrates were situated horizontally 4 cm away from the central line of the target and vertically 3.5 cm from the surface of the target. The solid state reaction process, described in our previous paper,[15] was adopted to make the target. The target was presputtered in the vacuum chamber with a mixture of Ar and O$_2$ for 20 h in order to homogenize the surface of the target prior to initiating film growth experiments. The target has also been presputtered for an additional 30 min to achieve the stable growth conditions necessary for each growth experiment. Nominal growth conditions were 50 W output power, 700 °C substrate temperature, total pressure varied from 35 to 200 mTorr, and 1:4 mixed O$_2$ to Ar ratio sputtering gas. For the dc growth experiment, the on-axis configuration was assumed and the chamber pressure ranged from 100 to 600 mTorr. The target composition was YBa$_2$Cu$_4$O$_8$; the other growth parameters were described in detail elsewhere.[15]

After deposition, we immediately introduced oxygen into the chamber. At the same time, the substrate temperature was cooled down to 450 °C, and maintained for 30 min under ambient oxygen atmosphere. Then the temperature was cooled down to room temperature. X-ray diffraction (XRD) was used to analyze the crystallinity and the phase of the as-grown films. The surface morphology of the films was observed by scanning electron microscopy (SEM). The thickness of the film was measured by profilometry, and this same technique was used to evaluate the deposition rate under various chamber pressures. The roughness and surface morphology of the films were examined by atomic force mi-
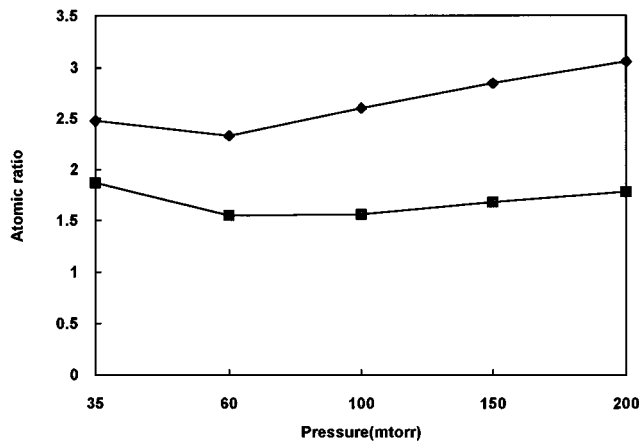
FIG. 1. Dependence of atomic ratio of (♦) Cu/Y and (■) Ba/Y on the total chamber pressure. Target composition was Y:Ba:Cu=1:2:3.

croscope (AFM). The electrical resistivity of each sample was measured by a four-probe technique. Finally, the composition of the metallic elements of the films was analyzed by inductively coupled plasma (ICP) emission spectroscopy.

III. RESULTS AND DISCUSSION

Figure 1 shows the ratios of Ba to Y and Cu to Y versus the chamber pressure. An increasing function of pressure above 60 mTorr was clearly seen but, below 60 mTorr, those ratios tended to decrease with pressure. We believe the reason for this was that the transport mechanisms of the sputtered particles in the sputtered gas during the whole pressure range were different. Helmer *et al.* have reported that the deposition rate (R), in a higher pressure range with diffusive transport of sputtered particles, is given by[20]

$$R = \frac{4Sh}{3L},\tag{1}$$

where S is the sputtered yield rate, h the mean free path of the transporting particles, and L the target to substrate distance. Since h varies with $1/p$, where p is the total chamber pressure, increasing the total pressure will reduce the deposition rate of all the metals or ions. It also means that the increase of scattering probabilities at higher pressures will decrease the target bombardment by the Ar ions and reduce the mean free path of the particles. This results in a reduction of sputtered particles arriving at the substrate and depositing on it, and thus minimizes the number of particles on the substrate. In our experiments above 60 mTorr pressure, in particular, the atomic ratios of Ba/Y and Cu/Y increased with total pressure, i.e., the reduction rate of Y species is larger than that of Ba and Cu while the pressure is increasing (Fig. 1).

In general, the modes of transportation of sputtered particles may be divided into three types, depending on chamber pressure.[20] At high pressures, the transportation of particles sputtered out by Ar ions is the diffusive mode, which can be characterized by simple gas phase diffusion. At low pressure, the transportation is ballistic and the sputtered atoms virtually never collide with gas atoms during transport. At inter-

mediate pressures, the form of transport is more complicated than in higher and lower pressure conditions. In this regime, the lighter sputtered species tend to suffer more loss of momentum and more direction-changing collisions than heavier species.[21–23] However, the threshold pressure at which a division of the borderlines of atoms occurred in various transportation modes remains uncertain, partly due to the initial high energy of sputtered atoms, and partly due to the differences of mass among sputtered atoms and gas atoms. The behavior of the multicomponent compound sputtering is more complicated because the components have different atomic radii, valence values, masses, and mean free paths. Consequently, over the last few years many researchers have used a trial and error method to fabricate superconducting films, and a certain range of exact conditions for growing the film has been found. But the reasons for this have seldom been studied. In this article, we derive empirical formulas by performing growth studies at various chamber pressures so as to provide a clear perspective and to reliably control multicomponent compound sputtering.

We assume that the deposition rate is not only inversely proportional to P, but also that it is influenced by other factors. These factors include the sticking coefficient, the valence values of sputtered particles, the difference of the resputtering effect by the negative oxygen ions or by secondary electrons, and the interactions among those particles with the growth chamber gas.[21] Under such an assumption, for each kind of sputtered particle above the threshold pressure of the diffusive transportation mode we can write

$$R = k \times P^{-a},\tag{2}$$

where k is a constant when all the other growth parameters are fixed, and the value of a indicates the degree of influence by the pressure. Each type of sputtered atom has a specific value, which is what we want to study and discuss. The larger the value of a, the higher the degree of influence on deposition rate by the pressure is.

The relative ratio values of Ba to Y ($R_{Ba/Y}$) and Cu to Y ($R_{Cu/Y}$) can be written as

$$R_{Ba/Y} = k_{Ba}/k_Y \times P^{(a_Y - a_{Ba})} = K_b \times P^b,\tag{3}$$

$$R_{Cu/Y} = k_{Cu}/k_Y \times P^{(a_Y - a_{Cu})} = K_c \times P^c.\tag{4}$$

The values of K_b, K_c, P^b, and P^c can be obtained by substituting the metallic compositional data from the ICP analysis into Eqs. (3) and (4). Figure 2 shows the plot of the relative deposition rate $R_{Cu/Y}$ and $R_{Ba/Y}$ versus the pressure by their natural logarithm forms. Figure 2 indicates a V-shaped outline on the $R_{Cu/Y}$ curve with the minimum around 60 mTorr. However, a U-shaped outline on the $R_{Ba/Y}$ curve was observed with a minimum range of 60–100 mTorr. The reason for this difference may be the different masses and scattering cross sections between Ba and Cu atoms. That is, the threshold pressures of the diffusive transportation mode for Ba and Cu atoms are different. The values of b and c can be obtained as 0.20 and 0.24, respectively, from the slopes of the straight lines at their diffusive regions in Fig. 2. The values of K_b and K_c were also obtained as -0.5 and -0.14 from the intercept of the both lines, respec-
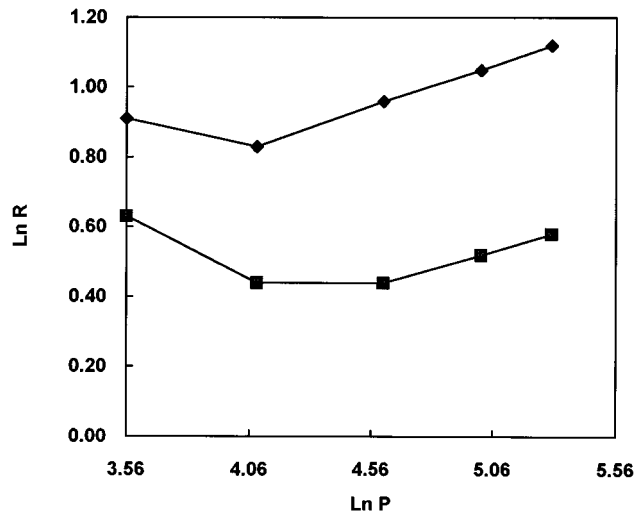
FIG. 2. Natural logarithmic plot of relative deposition ratio of (◆) Cu/Y and (■) Ba/Y of the rf sputtered thin films vs chamber pressure.
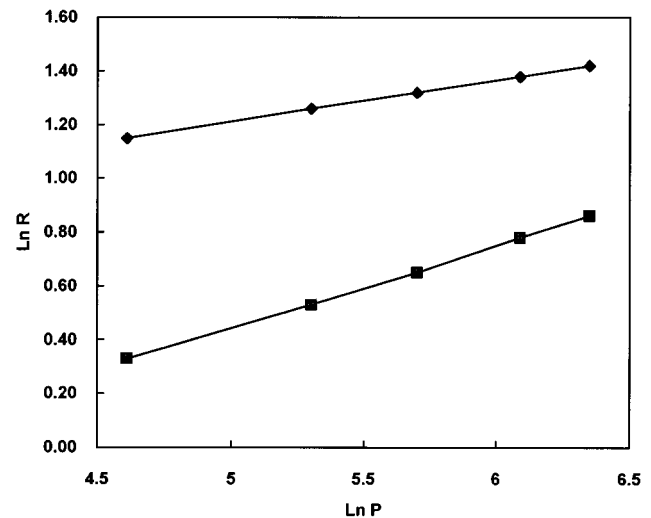

FIG. 3. Natural logarithmic plot of relative deposition ratio of (◆) Cu/Y and (■) Ba/Y of the dc sputtered thin films vs chamber pressure.

tively. These former two values imply that the changing rate of $R_{Cu/Y}$ versus P was larger than that of $R_{Ba/Y}$. Therefore, when the pressure was increased, the deposition rate of Ba must be less than that of Cu. In terms of the values of b and c, we know that a_Y is the largest of the three atoms, which indicates the strongest dependence on the deposition rate of the Y atom with the pressure among the three atoms. That is why the deposition rate of the Y atom was depressed more severely than that of Ba and Cu atoms when the pressure increased. Thus, the atomic ratios of Ba/Y and Cu/Y increase with increasing pressure. Our experimental results are different from others obtained by off-axis rf deposition,[24] which is to say, if the resputtering effect of the negative ion is avoided, the atomic ratio of the metallic composition of the films would be the same as the target. In our case, we believe that the conditions can satisfy the statements given in Ref. 24, as mentioned above, under the lower pressure. That is, the transportation of the sputtered particles was mostly in the ballistic mode.

In fact, the ejected particles are not simply inversely proportional to pressure, they also depend on the growth conditions and the kinds of sputtered atoms, which indicates that the simple form in Ref. 20 should be changed into an exponential form with different exponent values for various atoms. Therefore, we compare these results with those obtained from the dc on-axis sputtering growth[15] (see Fig. 3). Neither of the lines $R_{Cu/Y}$ and $R_{Ba/Y}$ show any concavity behavior because the chamber pressure begins at 100 mTorr in dc sputtering experiments, i.e., both of the transportation modes are in the diffusive form. Below 100 mTorr, the resputtering effect on Cu atoms by negative ion oxygen ions is very serious and does not fit any relation to total pressure. The values of b and c in Fig. 3 are 0.30 and 0.15, respectively. The value of a_{Cu} at the dc sputtering is larger than a_{Ba}, which means that the deposition rate of the Cu atoms is more seriously influenced by pressure than that of the Ba atoms.

These results are different from those of rf off-axis sputtering. There are two reasons that may explain the difference

between rf off-axis and dc on-axis sputtering. One is the resputtering of negative oxygen ions, and the other is the mass difference between Ba and Cu atoms. The different results produced by those two factors can be clearly distinguished by film fabrication under various system configurations. Since the vapor pressure of the Cu atom is the highest of the three atoms,[14] the bombardment of negative oxygen ions or secondary electrons will easily weaken the bonding of Cu–O and induce the resputtering effect. From our experimental data, the deposition ratio of the Cu atom to the Y atom in the dc sputtering system is less than in the rf sputtering system although the substrate temperature of the off-axis system is higher than that of on-axis system. Simultaneously, the initial target composition ratio of the Cu to the Y atom was 4 to 1, and the O$_2$ to Ar gas ratio (1:4) was also smaller than that of off-axis system, i.e., under the conditions described above for off-axis sputtering systems, the probability of resputtering the Cu atoms must be much higher than that in on-axis system; but, in fact, this was not the case. Because in the off-axis sputtering condition the negative ions cannot strike back onto the film, the resputtering effect of negative oxygen is one of the major factors behind this result. In addition, since the mass of the Ba atom is two times larger than that of the Cu atom, the large angle scattering probability of Cu by Ar ions during transportation to the substrate will be higher than that of the Ba atom. That was one of the possible reasons why the slope of c in the $R_{Cu/Y}$ curve was smaller than the value b of $R_{Ba/Y}$ in the on-axis dc sputter system. On the contrary, for off-axis sputtering, fewer Ba atoms arrived at the substrate parallel to the target surface due to the small potential for large angle scattering events. For Cu atoms, the probability of larger angle scattering was higher; therefore, in the off-axis configuration the value of c was larger than that of b. Due to the small difference between the value of b and c in off-axis rf sputtering, it seems that the resputtering effect is almost avoided in this case. The larger angle scatterings of Cu atoms and the minor resputtering effect in the off-axis system might be the primary factors that account for the value of c being a little larger than that
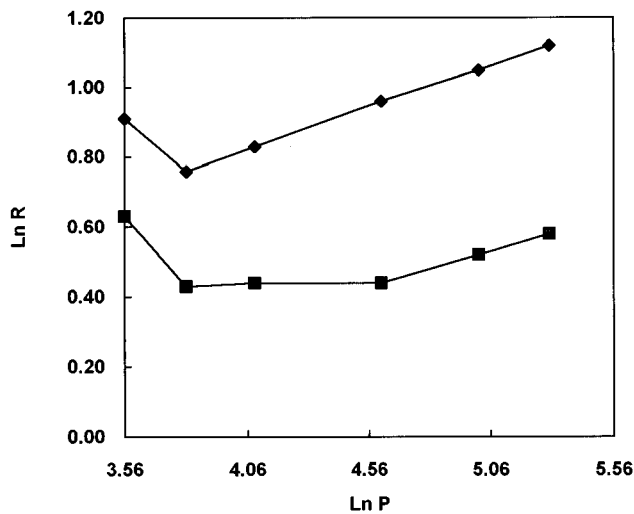
FIG. 4. A redrawing of Fig. 2 with additional data on the film that was fabricated at 45 mTorr pressure. (◆) Ln Cu/Y; (■) Ln Ba/Y.

of b in the off-axis case, or completely different, as in the case of the on-axis system.

Since we did not consider the effects of the sticking co-efficient of each atom, interactions between all kinds of par-ticles, or the valence values of ionized sputtered atoms, the above analysis seems to be a rough one. But the aim of our experiment is to utilize a simple model that does not involve complicated parameter settings. We also hope to shed some light on the fabrication by the sputtering of oxide supercon-ductors and to propose an empirical formula to describe and predict the composition of the as-deposited film in multicom-ponent (e.g., YBa$_2$Cu$_3$O$_7$) sputtering growth.

Our finding that the atomic ratio tends to change in pres-sures ranging from 60 to 35 mTorr is similar to the results of single target sputtering experiments made by Helmer *et al.*[20] Their deposition rate was not inversely proportional to the pressure if chamber pressures were below 10 mTorr. That is to say, the transportation of sputtered particles was not in the diffusive form. Therefore, it was natural for us to predict the existence of an intermediate region with a different transport mechanism from 35 to 60 mTorr, which we assume to be a mixed mode with ballistic and diffusive transportations. We performed another growth experiment at 45 mTorr chamber pressure to check this assumption. Figure 4 exhibits a plot redrawn from Fig. 2 together with this additional experimen-tal data. The experimental results indicate that the value of $R_{Ba/Y}$ at 45 mTorr is the same as that of $R_{Ba/Y}$ at 60 mTorr, but smaller than that of $R_{Ba/Y}$ at 35 mTorr, and that the value of $R_{Cu/Y}$ was smaller than those of $R_{Cu/Y}$ at 60 and 35 mTorr. We suggest that the transport of Ba atoms is almost in the intermediate region and that it exhibits a steady and pressure independent feature from 45 to 100 mTorr. But, for Cu at-oms, the transport was almost of the diffusive mode and partly of the ballistic mode, which was evidenced by a linear relationship with pressure in logarithmic form such as the situation above 60 mTorr. If the pressures were higher than 45 mTorr, the mode of transport would transfer to the diffu-sive mode. However, at pressures lower than 45 mTorr, the mode of transport will transfer to the ballistic mode. In the

intermediate regime, the concentration of the deposited atom contains two parts, one of which comes from the diffusive transport but has lower scattering probability, the other of which results from ballistic transportation, which will decay in the natural exponential form with pressure and target–substrate distance.[20] Thus the deposition ratio was higher at 35 mTorr than that at 60 mTorr.

If the pressures were not between 35 and 60 mTorr, all the films were fabricated under the diffusive mode of transpor-tation growth, and there were small ballistic components on the films. The higher the chamber pressure, the better the surface morphology and the homogeneity on the films. Ac-tually, SEM micrographs of the surface of the films demon-strate these expected results, shown in Figs. 5(a)–5(c). These figures clearly show that the films grown at lower chamber pressures exhibit rougher and more inhomogeneous surface morphology because they suffered from bombardments by higher energetic particles. The film surface was also found to be piled up with the same shape grains. When the chamber pressure is increased, the microstructure of the films be-comes smoother and more homogeneous, as shown in Fig. 5(c). This is because the level of energy of sputtered particles under diffusive mode transportation will be almost equal to that of local gas near the substrate region by thermalization processes.[25,26] Thus, if there were enough thermal energy on substrate and time periods, the particles on the substrate would gradually arrange themselves by migration. Therefore, when a higher energetic particle is ejected from the target regime without scattering collision, it is possible to make a defect or create a nonhomogeneous region on the film sur-face, or even possible to induce a new nucleation core, which would produce many grains on the surface as shown in Figs. 5(a) and 5(b), especially in Fig. 5(a), which is the most se-rious. The surface morphology of the thin film is very im-portant for the performance of microwave devices, especially for ring resonators, and this has been studied and reported in Ref. 27. Of course the roughness of the film surface, as shown in Figs. 6(a) and 6(b), would be different. The rough-ness is higher when the growing pressure is as low as 35 mTorr. It could become smaller if the pressure is increased, as demonstrated in Fig. 6(b). Figure 7 shows the root mean square (rms) roughness of the films versus various chamber pressures. At higher pressure conditions, the growth rate will be reduced by the scattering effect, and the transportation mode of the ejected particles will be thermalized into a dif-fusive mode; thus, there is more time to allow the atoms to order themselves and to decrease the ion bombardments on the film surface.[28] Therefore, the higher the chamber pres-sure, the smaller the roughness of the film was. Although the microstructures of the films are different, the phases of all the films almost always exhibit a c-axis preferred orientation, as shown in Fig. 8.

The deposition rate of thin film growth is proportional to the number of particles that arrive at the substrate. Moreover, the number of arrived particles is affected by the scattering from one another. Therefore, when the chamber pressure is higher, the probability of scattering is higher, which in turn reduces the number of arrived particles. For this reason, the growth rate of thin films decreased when the chamber pres-
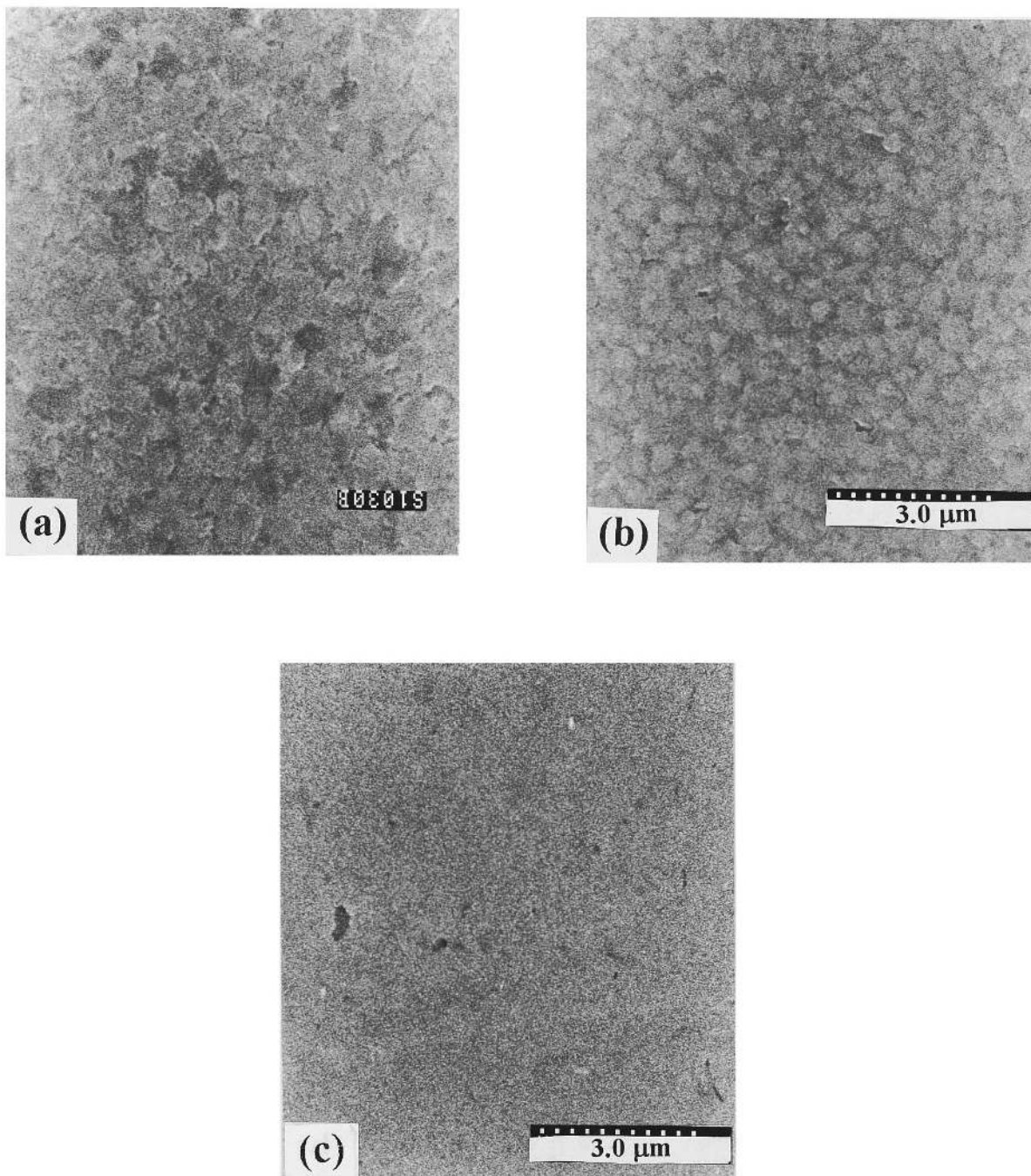
FIG. 5. SEM micrographs of the as-grown films surfaces. Films were deposited at 700 °C, 1/4 O$_2$–Ar ratio, 50 W output power, and various pressures: (a) 35, (b) 60, and (c) 150 mTorr.

sure was increased, as shown in Fig. 9. From Fig. 9, it is clearly seen that the deposition rate of 35 mTorr is three times larger than that of 200 mTorr, which indicates a much lower scattering probability of 35 mTorr than that of 200 mTorr. It seems meaningful to fit the data in Fig. 9 to $R = C_1 \exp(C_2 P)$ in the pressure range 35–100 mTorr, and to $R = C_3 P + C_4$ for pressure above 100 mTorr; the values of C_1, C_2, C_3, and C_4 were then 737.7, -0.0076, -1.8, and 530, respectively. These curve fitting results may support the above assumption that the ballistic mode of transportation of sputtered particles still exists at pressure lower than 100 mTorr. Moreover, from the two different kinds of curve fit-

tings in Fig. 9 at the 100 mTorr pressure point, we clearly demonstrate that there are two different major modes of transport mechanisms of sputtered particles in deposition growth. The transport was dominated by the ballistic mode below 100 mTorr pressures and showed an exponential form, but above 100 mTorr pressures it could be fitted by a linear form and demonstrated the diffusive mode of transportation. This result was found to coincide with information about the transportation of Ba atoms in Fig. 4. This result also supports the results of our dc growth experiments that demonstrate the superiority of the diffusive mode above the 100 mTorr chamber pressure.
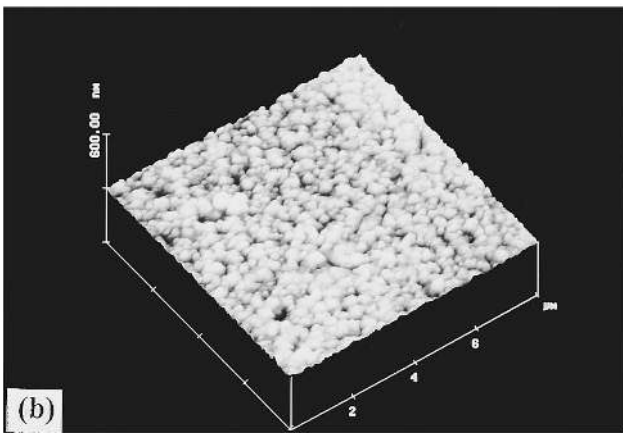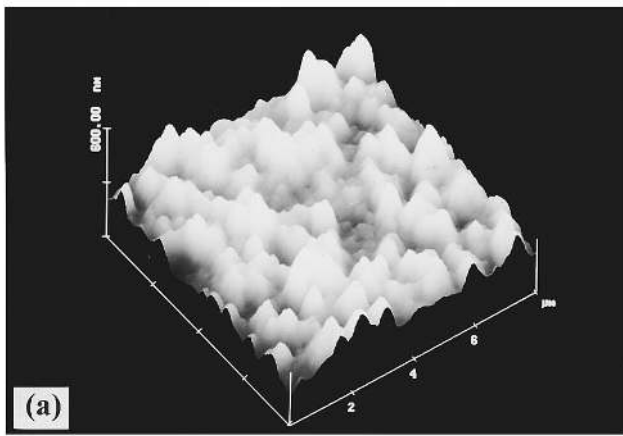
FIG. 6. AFM micrographs of the surfaces of the as-grown films fabricated at various pressures: (a) 35 and (b) 200 mTorr. The vertical axis is the height of the film surface, and the horizontal axis is the scanning range being examined.

The superconducting transition behavior and the T_c value of the films indicate various curves of resistance versus temperature (R-T) and the different values of the critical transition temperature, shown in Fig. 10. We expected that, when the growth chamber pressure was 35 mTorr, the surface of the film would be bombarded by more energetic particles,
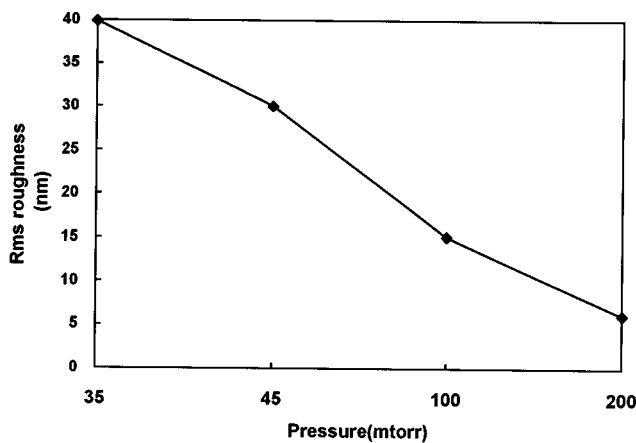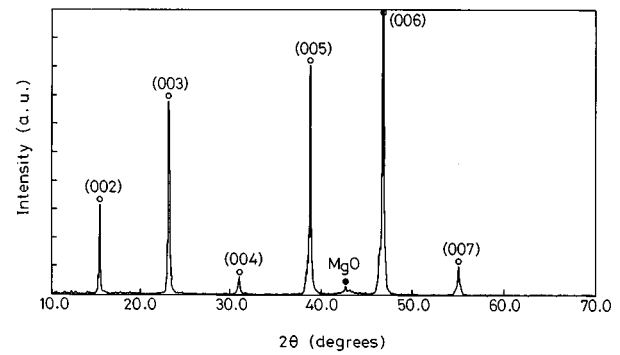

FIG. 8. XRD pattern of as-grown film deposited at 700 °C, 1/4 O$_2$–Ar ratio, 50 W output power, and 100 mTorr chamber pressure.

that induced the stress concentrated center which would easily cause the point defects or line defects or even result in nonordering and discontinuities in structure. Therefore, what may account for the two-step transition phenomena from the R-T curve, i.e., two phases simultaneously existed, one is the orthorhombic I phase with 90 K T_c and the other is the orthorhombic II phase with 60 K T_c.[29,30] The structure of the 90 K orthorhombic I phase is not continuous in the electrical conductivity path so the zero-resistance temperature (T_{co}) is only 60 K, as shown in Fig. 10(a). At 150 mTorr, the superconducting behavior of the electrical property is very simple and pure, as shown in Fig. 10(b), which indicates that the unique existence of the 90 K orthorhombic I phase with an 87 K T_{co} value. On the other hand, the superconducting behavior of the film grown at 200 mTorr was different from those described above, and demonstrated an unclear phase of orthorhombic I and exhibited T_{co} at 65 K, as shown in Fig. 10(c). The difference in superconducting properties between 200 and 35 mTorr pressure occurred at the transition shape of the orthorhombic I phase. The transition shape at 35 mTorr was sharper than at 200 mTorr. The reason for this difference may have to do with the different chamber pressures because

FIG. 7. Dependence of the roughness of the films on the total pressure.
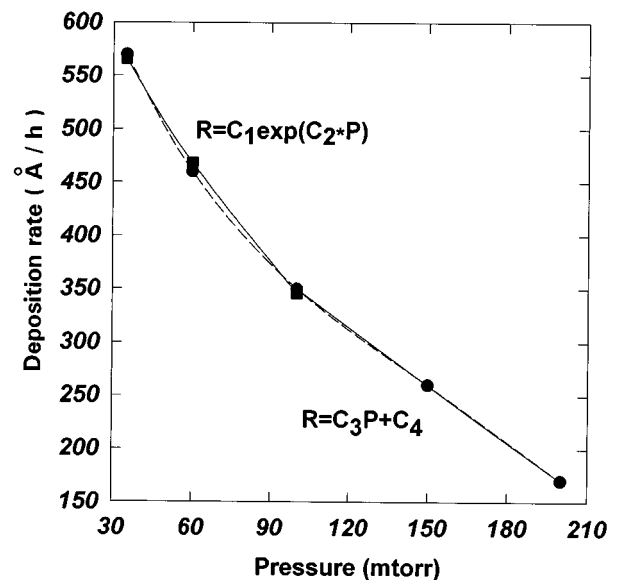

FIG. 9. Dependence of growth rate of the thin films on the total pressure. The solid line is a curve fitting result; the broken line is experimental data.
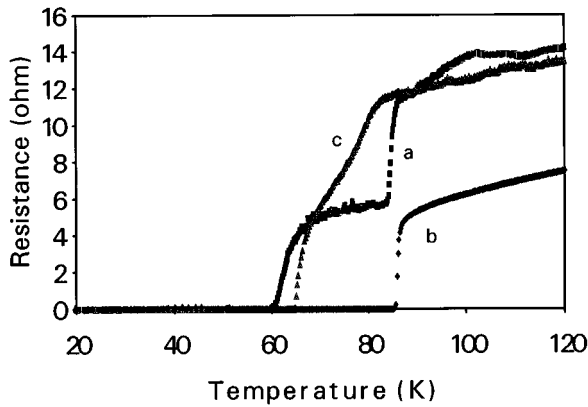
FIG. 10. Resistance-temperature curves of as-grown 123 thin films fabricated at (■) 35 mTorr, (♦) 150 mTorr, $R*10$, and (▲) 200 mTorr, $R*5$.
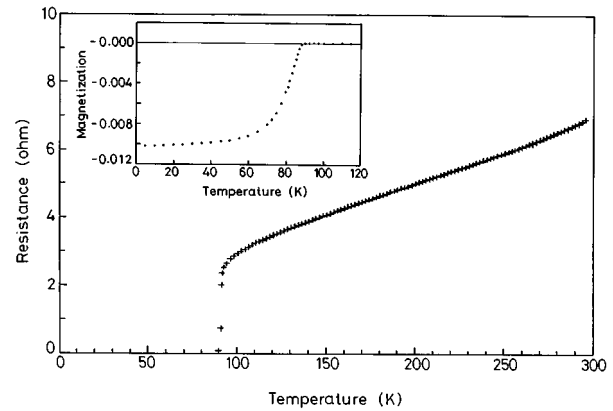

FIG. 11. Resistance-temperature curve of as-grown 123 thin film fabricated at 370 mTorr, and the temperature dependence ac susceptibility for the same sample (inset).

of the small nonhomogeneous structure and phase discontinuity resulting from the bombardment of high energetic particles in the surface of the film at higher pressure conditions. We also observed that the electrical properties of the film grown at 200 mTorr were not as good as those for the one grown at 150 mTorr, even though they were all based on the thermalization concept[25,26] during the diffusive transport mode. We believe that the noise level of the rf sputtering system rather than the pressure factor was the probable reason behind the difference in transition behavior. The noise of the rf system may be induced by the short circuit between the electrode of the heater and the chamber resulting from the crush of target crack or any conducting impurity. The effect of the short circuit was similar to the substrate biasing phenomenon that resulted in charged ion bombardment, and then induced resputtering and damage on the film surface.[31] Moreover, the energy of each sputtered particle was almost thermalized to equal the thermal energy of the local substrate region by scattering processes at higher pressures; the number of particles that arrived at the substrate was very limited. Under the greater noise level state, the metallic composition of the first few layers deviated from the exact stoichiometry of YBa$_2$Cu$_3$O$_7$, the arranged order of each metallic atom was also out of the periodic way, and the energy of the later particles was not high enough to support the atom migration and then diffuse to an exact position for rearranging themselves. In one case the defects induced at the beginning by ion bombardment were not able to moderate or be compensated for completely. This resulted in a feature of the transition curve, shown in Fig. 10(c), that has been explained by Kaneko *et al.*[32] and Matsubara *et al.*[33] From this, we suppose that raising the substrate temperature and minimizing the output noise level could fabricate films with the same quality as that grown at 150 mTorr under this 200 mTorr pressure condition, i.e., single phase in crystalline and pure single orthorhombic I phase in the as-grown films. As expected, the T_{co} value was as high as 82 K and the phase was pure when we raised the substrate temperature to 720 °C and reduced the output noise level.

In our lab, we have also fabricated films with 90 K T_c by off-axis sputtering, shown in Fig. 11, or by dc on-axis, as in Refs. 34 and 35, but, on obtaining the 90 K films, the growth

chamber pressure was 370 mTorr, and the substrate to target distance (horizontal distance 4 cm, vertical distance 3 cm) was also different from that described previously. Therefore, we do not include those results in these discussions.

We believe that the properties of critical current (J_c), surface resistance (R_s), and magnetic penetration depth (λ_H) are highly dependent on the quality of the superconductor. These relationships have been widely studied and discussed by other researchers.[36,37] Of course, it is interesting to speculate on the properties related to the material properties themselves, which were fabricated using various chamber pressures. But in this article, we prefer to focus on changing the composition of the metal elements, surface morphology, deposition rate, and the transition behavior and their T_c value in the films. Then we explain the relationship between the empirical formula of the deposition ratio of atoms and chamber pressure in terms of the mode of transportation of the ejected particles.

IV. CONCLUSION

From the above experiments and statements, it can be seen that the chamber pressure is a very important factor in controlling the exactly metallic composition of as-deposited films. Pressure also affects the microstructure and surface morphology of the films. Except in very low pressures, the velocities of diffusion for each particle will be different and must be taken into consideration. The metal composition will deviate from its stoichiometric condition due to the different deposition rate. In addition, the pressure effect will influence the growth rate and surface morphology. At higher pressures, the growth rate is low and the deposition time is longer and, hence, better surface morphology and structure homogeneity can be obtained. On the other hand, at lower pressures, the growth rate is higher but the homogeneity and morphology of the film is worse, which leads to bad electrical properties. From a series of experiments, we obtained the better quality film with 87 K T_{co} and $J_c > 10^5$ A/cm^2 at 77 K under conditions of 50 W output power, 1/4 mixed ratio of O$_2$ to Ar, 700 °C substrate temperature, and 150 mTorr chamber pres-

sure. In addition, films with T_c values of 90 K can still be obtained by just changing the substrate position and other parameters.

ACKNOWLEDGMENT

[1] P. Chaudhari, R. H. Koch, R. B. Laibowitz, T. R. Mcguire, and R. J. Gambino, Phys. Rev. Lett. **58**, 2684 (1987).

[2] J. Gao, Y. Z. Zhang, B. R. Zhao, P. Out, C. W. Yuan, and L. Li, Appl. Phys. Lett. **53**, 2675 (1988).

[3] M. L. Mandich *et al.*, Phys. Rev. B **38**, 5031 (1988).

[4] D. Dijkkamp *et al.*, Appl. Phys. Lett. **51**, 619 (1987).

[5] H. Abe, T. Tsuruoka, and T. Nakamori, Jpn. J. Appl. Phys. **27**, L1473 (1988).

[6] W. Y. Lee *et al.*, Thin Solid Films **166**, 181 (1988).

[7] R. L. Sandstrom *et al.*, Appl. Phys. Lett. **53**, 444 (1988).

[8] C. B. Eom *et al.*, Appl. Phys. Lett. **55**, 595 (1989).

[9] N. Newman *et al.*, Appl. Phys. Lett. **57**, 520 (1990).

[10] A. M. Kadin and P. H. Ballautine, IEEE Trans. Magn. **25**, 2437 (1989).

[11] D. J. Kester and R. Messier, J. Vac. Sci. Technol. A **4**, 496 (1986).

[12] J. J. Hanak and J. P. Pellicane, J. Vac. Sci. Technol. **13**, 406 (1976).

[13] J. J. Cuomo, R. J. Gambino, J. M. E. Harper, J. D. Kuptsis, and J. C. Webber, J. Vac. Sci. Technol. **15**, 281 (1978).

[14] T. J. Selinder, G. Larsson, U. Helmersson, and S. Rudner, J. Appl. Phys. **69**, 390 (1991).

[15] S. C. Wu, H. T. Hsu, F. H. Chen, W. R. Chang, and T. Y. Tseng, J. Mater. Sci. **29**, 5593 (1994).

[16] R. Schneider, J. Greek, G. Linker, O. Meyer, and R. Smithy, Physica C **220**, 165 (1994).

[17] K. Tanabe, D. K. Lathrop, S. E. Russek, and R. A. Buhrman, J. Appl. Phys. **66**, 3148 (1989).

[18] U. Poppe *et al.*, Solid State Commun. **66**, 661 (1988).

[19] C. B. Eom, J. K. Sun, Yamamoto, A. F. Marshall, K. E. Luther, and T. H. Geballe, Appl. Phys. Lett. **55**, 595 (1989).

[20] J. C. Helmer and C. E. Wickersham, J. Vac. Sci. Technol. A **4**, 408 (1986).

[21] S. M. Rossnagel, I. Yang, and J. J. Cromo, Thin Solid Films **59**, 199 (1991).

[22] R. R. Olson, M. E. King, and G. K. Wehner, J. Appl. Phys. **50**, 3677 (1979).

[23] W. D. Westwood, J. Vac. Technol. **15**, 1 (1978).

[24] N. Terada *et al.*, Jpn. J. Appl. Phys. **27**, 639 (1990).

[25] R. E. Somekh, J. Vac. Sci. Technol. A **2**, 1285 (1984).

[26] M. Turner, I. S. Falconer, B. W. James, and D. R. McKenzie, J. Appl. Phys. **65**, 3671 (1989).

[27] S. C. Wu *et al.*, Appl. Phys. Lett. **65**, 3281 (1994).

[28] G. A. C. Westerheim, L. S. Yu-Janes, and A. C. Anderson, IEEE Trans. Magn. **27**, 1001 (1991).

[29] J. M. Tarason, L. H. Green, W. R. McKinnon, G. W. Hulland, and T. H. Geballe, Science **235**, 1373 (1987).

[30] R. Beyers *et al.*, Physica C **162-164**, 548 (1989).

[31] See, for example, S. M. Rossnagel, in *Thin Film Processes II*, edited by J. L. Vossen and W. Kern (Academic, New York, 1991).

[32] N. Kaneko, T. Kawasaki, T. Motoi, and K. Yamamoto, Physica C **221**, 243 (1994).

[33] M. Matsubara, T. Morishita, and I. Hirabayashi, Appl. Phys. Lett. **64**, 1868 (1994).

[34] C. J. Huang, C. Y. Chang, M. C. Chen, and T. Y. Tseng, J. Am. Ceram. Soc. **74**, 2305 (1991).

[35] C. J. Huang, C. Y. Chang, and T. Y. Tseng, Physica C **185-189**, 2173 (1991).

[36] C. B. Eom *et al.*, Physica C **171**, 354 (1990).

[37] X. X. Xi *et al.*, IEEE Trans. Magn. **27**, 982 (1991).